

Gaussian process aided function comparison using noisy scattered data

Abhinav Prakash, Rui Tuo and Yu Ding

Department of Industrial and Systems Engineering, Texas A&M University.
3131 TAMU, College Station, TX 77843, USA

Abstract

This work proposes a new nonparametric method to compare the underlying mean functions given by two noisy datasets. The motivation for the work stems from an application of comparing wind turbine power curves. Wind turbine data present new problems, including that two different datasets do not share the same input points and individual datasets do not have replicates for the response at a given input point. Our proposed method estimates the underlying functions for different data samples using Gaussian process models. The posterior covariance is used to build a confidence band for the difference in the mean functions. Then, the band is used for hypothesis test as well as for identifying the regions of the input space where the functions are statistically different. This identification of difference regions is also distinct from many existing methods, which either simply conduct a hypothesis test without identifying regions of difference or provide only a point estimate (metric) of the overall functional difference. Practically, understanding the difference regions can lead to further insights and help devise better control and maintenance strategies for the turbine. The merit of our proposed method is demonstrated by using three simulation studies and four real wind turbine datasets.

Keywords: Function comparison, Hypothesis test, Gaussian process, Uncertainty quantification

1 Introduction

Comparing information from two datasets is an important topic in statistics. Various methods exist to compare datasets arising from univariate distributions (e.g. two sample t -test (Fisher, 1925)), and multivariate distributions (e.g. Hotelling's T^2 test (Hotelling, 1931)). The literature is not just limited to comparing finite dimensional objects, but also extends to functions. In this work, we

propose a new nonparametric method to compare functions. Our work is motivated by an application in wind energy sector, in which the goal is to compare power curves of two wind turbines. Power curve of a wind turbine is a function with wind power as output, and the environmental variables (wind speed, wind direction, air density etc.) as inputs. Power curves are used to characterize the performance of wind turbines (IEC, 2005). Hence, comparing power curves plays a critical role in turbine performance comparison and benchmarking, helping identify better designs and best practice (Hwangbo et al., 2017). One key feature of the datasets arising from wind turbines, however, is that the input conditions (e.g. wind speed or wind direction) for the observations cannot be controlled. Hence, the input points for any two datasets are not the same. Another aspect of the data is the lack of replicates for any input point.

The problem of testing the equality of two nonparametric functions has been studied extensively in the literature. One early work is Hall and Hart (1990). They defined a test statistic for the problem using the smoothed (estimated) function values and obtained a distribution of their test statistic using bootstrap method. King et al. (1991) also studied the same problem using smoothing techniques, and proposed an exact distribution for their test statistic under the normality assumption for the errors. Delgado (1993) proposed another test statistic using marked empirical process. Without using the smoothing technique, their method thus made the test independent of the choice of smoothing parameter. Fan and Lin (1998) worked on reducing the dimension of the problem using discrete Fourier transforms so that standard multivariate techniques can be used to test the hypothesis. All the papers described hitherto assume identical input points for the datasets in comparison. This assumption may not be valid as in the case of wind turbines described earlier. Kulasekera (1995), Kulasekera and Wang (1997), Munk and Dette (1998), Neumeyer and Dette (2003) proposed tests which are valid under different input points among the datasets, but all the methods above provide a binary answer of whether the functions are statistically the same or not. They do not provide any insights on the regions of the input space where the functions are different, or which function has higher or lower function values. Cox and Lee (2008) addressed this problem, using a pointwise testing procedure based on the Westfall-Young randomization (Westfall and Young, 1993) that identifies the regions of the input space where the functions are different. However, Cox

and Lee’s method is based on the same set of input points, and also requires replicates of the response at each input point.

In this work, we propose a new method to compare functions. The proposed method tests the null hypothesis that the functions are equal at all input points. When the null hypothesis is rejected, the proposed method can provide the region in the input space where the functions in comparison are different. The method does not require the input points among the samples to be the same, nor does it need replicates of the observations. Our method partially adopts a Bayesian framework, for we control the type I error based on a GP prior for the underlying function. That Gaussian process (GP) regression works for a large class of functions makes this method applicable to many problems. Gaussian process models also provide uncertainty quantification, enabling a statistically reliable function comparison.

In the proposed method, we first use a GP regression model to recover the functions from the noisy datasets. We then build a confidence band, given a prescribed type-I error, on the difference between the functions throughout the input space under the null hypothesis. If the actual difference between the functions computed using the data is beyond the confidence band, we reject the null hypothesis. We call the method *function comparison using Gaussian Process* or **funGP**. Although we assume the functions as realizations of GPs, we demonstrate that the method works well even for deterministic functions. We also apply our method to real wind turbine datasets, and compare our method with some existing work for turbine performance characterization.

We organize the rest of the paper as follows. We provide the details of the proposed method in Section 2. We present the simulation examples in Section 3. We apply the funGP method in Section 4 to wind turbine datasets. We conclude the work with some discussions in Section 5.

2 The funGP Method

In this section, we describe the mathematical formulation and the implementation details of the proposed funGP method.

2.1 Problem Formulation

Let us consider two datasets, $\{\mathcal{D}_i \mid i = 1, 2\}$, with n_1 and n_2 data points, respectively. Each data point of both datasets consists of a d -dimensional input vector and a real-valued output. Assume that \mathcal{D}_1 can be denoted by an ordered pair $\{\mathbf{X}^{(1)}, \mathbf{y}^{(1)}\}$, where $\mathbf{X}^{(1)}$ is a $n_1 \times d$ matrix with each row corresponding to input variable values for one data point and $\mathbf{y}^{(1)}$ is a vector of length n_1 with each component as response for one data point. Similarly \mathcal{D}_2 can be denoted as $\{\mathbf{X}^{(2)}, \mathbf{y}^{(2)}\}$. Specifically,

$$\mathbf{y}^{(1)} = \begin{bmatrix} y_{11} \\ y_{12} \\ \vdots \\ y_{1n_1} \end{bmatrix}, \quad \mathbf{X}^{(1)} = \begin{bmatrix} -\mathbf{x}_{11}^\top - \\ -\mathbf{x}_{12}^\top - \\ \vdots \\ -\mathbf{x}_{1n_1}^\top - \end{bmatrix}, \quad \mathbf{y}^{(2)} = \begin{bmatrix} y_{21} \\ y_{22} \\ \vdots \\ y_{2n_2} \end{bmatrix}, \quad \mathbf{X}^{(2)} = \begin{bmatrix} -\mathbf{x}_{21}^\top - \\ -\mathbf{x}_{22}^\top - \\ \vdots \\ -\mathbf{x}_{2n_2}^\top - \end{bmatrix}.$$

We also assume that these datasets come from underlying models given by:

$$y_{ij} = f_i(\mathbf{x}_{ij}) + \epsilon_{ij}, \quad i = 1, 2, \quad j = 1, \dots, n_i,$$

where $f_1(\cdot)$ and $f_2(\cdot)$ are two smooth continuous functions with the same domain of $\mathcal{X} \subseteq \mathbb{R}^d$ and $\epsilon_{ij} \stackrel{iid}{\sim} \mathcal{N}(0, \sigma_\epsilon^2)$ with the constant $\sigma_\epsilon^2 < \infty$ as the variance of the noise. We here consider the same noise variance for both datasets. This assumption is introduced only for simplicity and can be relaxed.

The goal is to test the following null and alternative hypotheses. The null hypothesis is that the functions are identical, whereas the alternative hypothesis is that the functions are different for at least one $\mathbf{x} \in \mathcal{X}$. Under the null hypothesis, H_0 :

$$f_1(\mathbf{x}) = f_2(\mathbf{x}) \quad \forall \mathbf{x} \in \mathcal{X}.$$

And, under the alternative hypothesis, H_1 :

$$\exists \mathbf{x} \in \mathcal{X} \quad s.t. \quad f_1(\mathbf{x}) \neq f_2(\mathbf{x}).$$

If we suppose that the datasets under comparison have the same set of input points, i.e. $\mathbf{X}^{(2)} = \mathbf{P}\mathbf{X}^{(1)}$, where \mathbf{P} is a permutation matrix, and if we also suppose that we have replicates for the response for all the input points, then any of the methods described in Section 1 can be used for the hypothesis testing to get a binary answer (yes/no) on the difference. Some of the methods can work even when the two datasets under comparison do not share the same input points (Kulasekera, 1995, Kulasekera and Wang, 1997, Munk and Dette, 1998, Neumeier and Dette, 2003), but they still provide the binary answer and not the regions of statistical difference. Cox and Lee (2008) would provide the regions of statistical difference apart from the binary answer, but only when we have the same input points and replicates.

When comparing two power curves of wind turbines, however, one cannot satisfy the conditions of the same input points and replicates at each input point. The input variable—wind speed—itself is random, and thus, getting the same sets of input points in two datasets is impossible. Also, we get only one response at one input location, which prohibits the use of a method that requires replicates. This application motivated us to devise a method requiring neither identical input points nor replicates, and can still provide the regions of statistical difference in the input space.

2.2 Hypothesis testing with a GP prior

The general idea for a hypothesis testing is to find a test statistic, and subsequently have a decision rule to either accept or reject the null hypothesis based on the value of test statistic. In the application described, we are not only interested in the binary answer that whether the two functions in comparison are different, we also want to understand where the difference lies in the input space. This requires us to obtain a test statistic at input points for which we do not have any data. We also assume that the input points for the two datasets are not the same. Thus, we would have to assume some structure in the functions (such as the functions are smooth and continuous) in order to recover the functions, and estimate the noise in the model. Here we adopt a Bayesian idea that imposes a prior structure on the functions. Specifically, we use a GP prior. So, the hypothesis testing is conditioned on the GP, and the type I error in the current context is defined as $\mathbb{P}_{GP}(H_0 \text{ is rejected} | H_0)$, where \mathbb{P}_{GP} denotes the probability measure given by the Gaussian process prior and H_0 denotes the

null hypothesis.

Let us assume that the functions $f_1(\cdot)$ and $f_2(\cdot)$ are samples from a GP with zero mean and a covariance function given by $k(\mathbf{x}, \mathbf{x}')$. The zero mean assumption is for mathematical simplicity, and we can assume a different mean function if necessary. Under the null hypothesis, the functions $f_1(\cdot)$ and $f_2(\cdot)$ are identical, considered as realizations from the same GP. Therefore, we use the same prior for both datasets. We define a cross-covariance matrix $\mathbf{K}(\mathbf{X}, \mathbf{X}')$ between a pair of input variable matrix \mathbf{X} and \mathbf{X}' , and a covariance vector $\mathbf{r}(\mathbf{x})$ between the input data \mathbf{X} and any point \mathbf{x} as follows:

$$\mathbf{K}(\mathbf{X}, \mathbf{X}') = \begin{bmatrix} k(\mathbf{x}_1, \mathbf{x}'_1) & k(\mathbf{x}_1, \mathbf{x}'_2) & \dots & k(\mathbf{x}_1, \mathbf{x}'_n) \\ k(\mathbf{x}_2, \mathbf{x}'_1) & k(\mathbf{x}_2, \mathbf{x}'_2) & \dots & k(\mathbf{x}_2, \mathbf{x}'_n) \\ \vdots & \vdots & \ddots & \vdots \\ k(\mathbf{x}_m, \mathbf{x}'_1) & k(\mathbf{x}_m, \mathbf{x}'_2) & \dots & k(\mathbf{x}_m, \mathbf{x}'_n) \end{bmatrix}, \quad \mathbf{r}(\mathbf{x}) = \begin{bmatrix} k(\mathbf{x}_1, \mathbf{x}) \\ k(\mathbf{x}_2, \mathbf{x}) \\ \vdots \\ k(\mathbf{x}_m, \mathbf{x}) \end{bmatrix}, \quad (1)$$

where $\mathbf{x}_1 \dots \mathbf{x}_m$ are the vectors in the rows of the matrix \mathbf{X} , and $\mathbf{x}'_1 \dots \mathbf{x}'_n$ are the vectors in the rows of the matrix \mathbf{X}' . When $\mathbf{X} = \mathbf{X}'$, \mathbf{K} is then a symmetric covariance matrix. Then, the predictive mean function for $f_1(\cdot)$ given \mathcal{D}_1 , and that for $f_2(\cdot)$ conditioned on \mathcal{D}_2 , are as follows:

$$\hat{f}_1(\mathbf{x}) = \mathbf{r}_1(\mathbf{x})^\top [\mathbf{K}(\mathbf{X}^{(1)}, \mathbf{X}^{(1)}) + \sigma_\epsilon^2 \mathbf{I}_{n_1}]^{-1} \mathbf{y}^{(1)}, \quad (2)$$

$$\hat{f}_2(\mathbf{x}) = \mathbf{r}_2(\mathbf{x})^\top [\mathbf{K}(\mathbf{X}^{(2)}, \mathbf{X}^{(2)}) + \sigma_\epsilon^2 \mathbf{I}_{n_2}]^{-1} \mathbf{y}^{(2)}, \quad (3)$$

where $\mathbf{r}_1(\mathbf{x})$ is the covariance vector between $\mathbf{X}^{(1)}$ and any point \mathbf{x} , $\mathbf{K}(\mathbf{X}^{(1)}, \mathbf{X}^{(1)})$ is the covariance matrix for $\mathbf{X}^{(1)}$, and \mathbf{I}_{n_1} is the identity matrix of proper size— $n_1 \times n_1$ in this case. The notations in Equation (3) are likewise defined. The predictive mean functions given in Equations (2) and (3) are, respectively, the best linear unbiased predictor (BLUP) for $f_1(\cdot)$ and $f_2(\cdot)$. For more details on use of GP models for regression, please see Rasmussen and Williams (2006).

We want to compare the functions $f_1(\cdot)$ and $f_2(\cdot)$ at all points in \mathcal{X} . This is practically intractable, as for any continuous function, there are infinitely many points in the domain. Hence, we test our

hypothesis on a dense regular grid $\mathcal{T} \subset \mathcal{X}$. Let us assume that the number of test points in \mathcal{T} is n_{test} . Testing on this regular grid is a reasonable approximation to testing for all $\mathbf{x} \in \mathcal{X}$ because of our underlying assumption that the functions are continuous and smooth. Let us define a matrix \mathbf{X}_{test} such that each row of the matrix represents one test point in \mathcal{T} . We can denote the predictive mean vector for all the points in \mathcal{T} as follows:

$$\begin{aligned}\hat{\mathbf{f}}_1 &= \mathbf{K}(\mathbf{X}_{test}, \mathbf{X}^{(1)})[\mathbf{K}(\mathbf{X}^{(1)}, \mathbf{X}^{(1)}) + \sigma_\epsilon^2 \mathbf{I}_{n_1}]^{-1} \mathbf{y}^{(1)}, \\ \hat{\mathbf{f}}_2 &= \mathbf{K}(\mathbf{X}_{test}, \mathbf{X}^{(2)})[\mathbf{K}(\mathbf{X}^{(2)}, \mathbf{X}^{(2)}) + \sigma_\epsilon^2 \mathbf{I}_{n_2}]^{-1} \mathbf{y}^{(2)},\end{aligned}\tag{4}$$

where $\hat{\mathbf{f}}_1 = (\hat{f}_1(\mathbf{x}_1) \dots \hat{f}_1(\mathbf{x}_{n_{test}}))^\top$, and $\hat{\mathbf{f}}_2 = (\hat{f}_2(\mathbf{x}_1) \dots \hat{f}_2(\mathbf{x}_{n_{test}}))^\top$.

Denote by a random vector \mathbf{G} the difference in the predictive mean for all the test points. Under the null hypothesis, $\mathbb{E}[\mathbf{G}] = \mathbf{0}$. With a little effort (see Appendix A.1 for details), we can find that the covariance of \mathbf{G} , denoted by $\mathbf{C}(\mathbf{X}_{test}, \mathbf{X}_{test})$, can be expressed as follows:

$$\begin{aligned}\mathbf{C}(\mathbf{X}_{test}, \mathbf{X}_{test}) &= \mathbf{K}(\mathbf{X}_{test}, \mathbf{X}^{(2)})[\mathbf{K}(\mathbf{X}^{(2)}, \mathbf{X}^{(2)}) + \sigma_\epsilon^2 \mathbf{I}_{n_2}]^{-1} \mathbf{K}(\mathbf{X}_{test}, \mathbf{X}^{(2)})^\top \\ &+ \mathbf{K}(\mathbf{X}_{test}, \mathbf{X}^{(1)})[\mathbf{K}(\mathbf{X}^{(1)}, \mathbf{X}^{(1)}) + \sigma_\epsilon^2 \mathbf{I}_{n_1}]^{-1} \mathbf{K}(\mathbf{X}_{test}, \mathbf{X}^{(1)})^\top \\ &- 2 \mathbf{K}(\mathbf{X}_{test}, \mathbf{X}^{(2)})[\mathbf{K}(\mathbf{X}^{(2)}, \mathbf{X}^{(2)}) + \sigma_\epsilon^2 \mathbf{I}_{n_2}]^{-1} \mathbf{K}(\mathbf{X}^{(2)}, \mathbf{X}^{(1)}) [\mathbf{K}(\mathbf{X}^{(1)}, \mathbf{X}^{(1)}) + \sigma_\epsilon^2 \mathbf{I}_{n_1}]^{-1} \mathbf{K}(\mathbf{X}_{test}, \mathbf{X}^{(1)})^\top.\end{aligned}\tag{5}$$

Under a GP model, the predictive mean follows a normal distribution. Thus, under the null hypothesis, the difference in the predictive means follows a multivariate normal distribution given by:

$$\mathbf{G} \sim \mathcal{N}(\mathbf{0}, \mathbf{C}(\mathbf{X}_{test}, \mathbf{X}_{test})).$$

Denote by \mathbf{g} the actual difference in the predictive means obtained using datasets \mathcal{D}_1 and \mathcal{D}_2 , meaning that under the null hypothesis, \mathbf{g} is a realization of the random vector \mathbf{G} . Our hypothesis testing reduces to checking whether \mathbf{g} can be a realization from \mathbf{G} . In order to control the type I error at a nominal level α , we would need to build a $1 - \alpha$ confidence band on \mathbf{G} . We then check whether \mathbf{g} remains within the band for all the values of $\mathbf{x} \in \mathcal{T}$. If there exists an \mathbf{x} for which the

difference, \mathbf{g} , is outside the confidence band then we reject the null hypothesis. The question is how to efficiently build the confidence band for the test grid of \mathcal{T} .

2.3 Building the confidence band

In order to build the $1 - \alpha$ confidence band on \mathbf{G} , we need to sample from a set with a coverage probability of $1 - \alpha$. For achieving that goal, we employ the Karhunen Loève (KL) expansion. KL expansion for a zero mean Gaussian process is given as follows:

$$g(\mathbf{x}) = \sum_{k=1}^{\infty} \sqrt{\lambda_k} \phi_k(\mathbf{x}) z_k,$$

where $\{z_k\}_{k=1}^{\infty}$ are uncorrelated standard normal random variables, $\{\phi_k(\cdot)\}_{k=1}^{\infty}$ are the basis functions, $\{\lambda_k\}_{k=1}^{\infty}$ are the eigenvalues. Given a finite number of n_{test} points, we do a truncated KL expansion of \mathbf{G} at any point $j \in \{1 \dots n_{test}\}$ in the following way:

$$(\mathbf{G})_j = \sum_{k=1}^{n_{test}} \sqrt{\lambda_k^{mat}}(\mathbf{u}_k)_j z_k,$$

where, λ_k^{mat} are the eigenvalues of the covariance matrix $\mathbf{C}(\mathbf{X}_{test}, \mathbf{X}_{test})$, \mathbf{u}_k are the normalized unit eigenvectors of the covariance matrix $\mathbf{C}(\mathbf{X}_{test}, \mathbf{X}_{test})$. We write the truncated KL expansion of \mathbf{G} for all the points in \mathcal{T} using the matrix notation as follows:

$$\mathbf{G} = \mathbf{U} \mathbf{\Lambda}^{\frac{1}{2}} \mathbf{z}, \tag{6}$$

where \mathbf{U} is a matrix with the eigenvectors of covariance matrix, $\mathbf{C}(\mathbf{X}_{test}, \mathbf{X}_{test})$, as its columns, $\mathbf{\Lambda}$ is a diagonal matrix having the eigenvalues of $\mathbf{C}(\mathbf{X}_{test}, \mathbf{X}_{test})$ as its diagonal elements, and \mathbf{z} is a vector of length n_{test} with uncorrelated standard normal random variables as its components; please see Appendix A.2 for further details on KL expansion.

In Equation (6), the randomness is introduced by \mathbf{z} . Hence, in order to build a $1 - \alpha$ confidence band on \mathbf{G} , we need to build the same level confidence band on \mathbf{z} , which can be constructed using the distribution of \mathbf{z} as follows. We know that for an n -dimensional uncorrelated standard normal

vector, a confidence region \mathcal{R} , with probability $\mathbb{P}(\mathcal{R}) = 1 - \alpha$, can be described using a hypersphere of radius r . This radius can be expressed as $r = \|\mathbf{z}\|$, where $\|\cdot\|$ is the ℓ_2 norm. The sum of squares of n uncorrelated standard normal follows a chi-square distribution with n degrees of freedom, i.e.,

$$r^2 = z_1^2 + z_2^2 + \dots + z_{n_{test}}^2 \sim \chi_{n_{test}}^2.$$

Hence r is computed by inverting the CDF of a chi-square distribution in the following way:

$$r = \sqrt{F_{n_{test}}^{-1}(1 - \alpha)}, \quad (7)$$

where $F_{n_{test}}^{-1}(\cdot)$ is the inverse CDF of $\chi_{n_{test}}^2$. Once we have the radius r , we sample \mathbf{z} from the region with a coverage probability of $1 - \alpha$ using the following rule:

- sample z_i from $\mathcal{N}(0, 1) \mid i \in \{1 \dots n_{test}\}$,
- if $\sum_{i=1}^{n_{test}} z_i^2 \leq r^2$, accept $\mathbf{z} = (z_1, z_2, \dots, z_{n_{test}})^\top$; else, reject.

We sample a large number (say 1,000) of \mathbf{z} from the confidence set and construct the confidence band for \mathbf{G} through:

$$\begin{aligned} \mathbf{ub} &= \text{Max}_{\mathbf{z}} \mathbf{U} \mathbf{\Lambda}^{\frac{1}{2}} \mathbf{z}, \\ \mathbf{lb} &= \text{Min}_{\mathbf{z}} \mathbf{U} \mathbf{\Lambda}^{\frac{1}{2}} \mathbf{z}, \end{aligned} \quad (8)$$

where \mathbf{ub} is the vector of upper bounds and \mathbf{lb} is the vector of lower bounds for the confidence band. We accept the null hypothesis H_0 at the confidence level of $1 - \alpha$, if the value of \mathbf{g} is everywhere within the band, i.e.

$$(\mathbf{lb})_j \leq (\mathbf{g})_j \leq (\mathbf{ub})_j \quad \forall j = 1 \dots n_{test},$$

where the notation $(\mathbf{a})_j$ is the j^{th} component of a vector \mathbf{a} . Similarly, we reject the null hypothesis at the $1 - \alpha$ confidence level if there is at least one violation, i.e.,

$$\exists j \in \{1 \dots n_{test}\} \text{ s.t. } (\mathbf{g})_j \notin [(\mathbf{lb})_j, (\mathbf{ub})_j].$$

If the eigenvalues decay rapidly, which is generally the case for a smooth Gaussian process, we can further reduce the computation cost for getting the band for \mathbf{G} . If the eigenvalues after m largest eigenvalues are close to zero, they do not contribute much for the band calculation. Hence, we can consider only the m largest eigenvalues. Doing so also reduces the length of \mathbf{z} , and we can recompute the radius of the confidence region. Let $\bar{\mathbf{U}}$ be $n_{test} \times m$ matrix whose columns are the eigenvectors corresponding to the m largest eigenvalues. Let $\bar{\mathbf{\Lambda}}$ be an $m \times m$ diagonal matrix with the m largest eigenvalues, and $\bar{\mathbf{z}}$ be a vector of length m of uncorrelated standard normal random variables. Then,

$$\begin{aligned} \mathbf{ub} &\approx \text{Max}_{\bar{\mathbf{z}}} \bar{\mathbf{U}} \bar{\mathbf{\Lambda}}^{\frac{1}{2}} \bar{\mathbf{z}}, \\ \mathbf{lb} &\approx \text{Min}_{\bar{\mathbf{z}}} \bar{\mathbf{U}} \bar{\mathbf{\Lambda}}^{\frac{1}{2}} \bar{\mathbf{z}}. \end{aligned}$$

In practice, we decide the value of m based on the rate of decay of the eigenvalues and a threshold. It is worth noting that we are getting an approximate band because of using a truncated KL expansion and by further taking only a subset of largest m eigenvalues. This may result in losing some confidence on the test. In other words, the probability of the confidence band would be less than $1 - \alpha$. A possible compensation can be made by setting a slightly higher confidence level than the nominal level.

2.4 Estimating the hyperparameters

Until now, we have assumed the values of the hyperparameters of the covariance matrix and the nugget σ_ϵ are known. Next, we describe the method we use to estimate these hyperparameters.

Let us assume that $\boldsymbol{\theta}$ is the vector containing all the hyperparameters of the covariance function and the nugget σ_ϵ . We estimate these hyperparameters by jointly maximizing the likelihood for both datasets \mathcal{D}_1 and \mathcal{D}_2 as follows:

$$\hat{\boldsymbol{\theta}} = \arg \max \mathcal{L}(\boldsymbol{\theta}; \mathcal{D}_1) + \mathcal{L}(\boldsymbol{\theta}; \mathcal{D}_2). \quad (9)$$

Having all the pieces together, we now formally state the algorithm for funGP.

Algorithm 1: funGP: function comparison using Gaussian process

Input: $\mathcal{D}_1 = \{\mathbf{X}^{(1)}, \mathbf{y}^{(1)}\}$, $\mathcal{D}_2 = \{\mathbf{X}^{(2)}, \mathbf{y}^{(2)}\}$, \mathbf{X}_{test} , α

Procedure:

- 1: Choose a covariance function.
- 2: Estimate the hyperparameters for the covariance function and the nugget, σ_ϵ , by optimizing the likelihood function given in Equation (9).
- 3: Compute the predictive mean $\hat{\mathbf{f}}_1$ for test points \mathbf{X}_{test} using \mathcal{D}_1 , and the predictive mean $\hat{\mathbf{f}}_2$ using \mathcal{D}_2 using Equation (4).
- 4: Compute the difference between predictive means, $\mathbf{g} = \hat{\mathbf{f}}_2 - \hat{\mathbf{f}}_1$.
- 5: Compute the matrix $\mathbf{C}(\mathbf{X}_{test}, \mathbf{X}_{test})$ given in Equation (5).
- 6: Do the eigen decomposition of $\mathbf{C}(\mathbf{X}_{test}, \mathbf{X}_{test})$ and store the eigenvalues in a diagonal matrix $\mathbf{\Lambda}$ and the corresponding eigenvectors in a matrix \mathbf{U} .
- 7: Compute the radius, r , of a standard normal vector of dimension n_{test} with a coverage probability of $1 - \alpha$ using Equation (7).
- 8: Sample a large number (say 1,000) of standard normal vector \mathbf{z} such that $\|\mathbf{z}\| \leq r$.
- 9: Compute the vector of upper bounds, \mathbf{ub} , and lower bounds, \mathbf{lb} , for all the test points using Equation (8).

Output:

If $(\mathbf{lb})_j \leq (\mathbf{g})_j \leq (\mathbf{ub})_j \quad \forall j = 1 \dots n_{test}$, functions are same at $1 - \alpha$ confidence level.

Else, functions are different at $1 - \alpha$ confidence level.

3 Simulation Study

In this section, we present three simulation studies for the funGP method. The goal is to estimate the type I and the type II errors. Because the type II error depends on the actual difference in the functions, we estimate the type II error for some small perturbations made to functions. In order to quantify the difference between a function and its perturbation, we use an L_2 distance percentage defined as follows:

$$L_2 \text{ dist } \% = \frac{\|f - g\|_{L_2}}{\|f\|_{L_2}} \times 100,$$

where f is the underlying function, and g is its perturbation.

In the first simulation study, the functions used are samples from a known Gaussian process. In the funGP method, we assume that functions can be modeled as realizations from Gaussian processes. But, in practice we need to know the exact covariance function form. In this case study, we use a known covariance function form, and thus, there is no misspecification of the covariance function form.

The other two case studies are based on some parametric functions available in the literature. In these two case studies, we do not know the exact covariance form to recover the functions as GP realizations. This is often the case in any application. Thus, we use a parametric covariance function as a surrogate for the true covariance. This will give us an idea of how the method fares when there is a potential model misspecification. In order to generate the datasets, we sample two sets of points from the input domain of the functions randomly. We then generate response by adding some i.i.d Gaussian noise to the evaluated function values at those input points.

In all the simulation studies, we use a constant mean, a squared exponential form for the covariance function, and a 95% confidence band, i.e. $\alpha = 0.05$. We conduct 1,000 runs to estimate the type I and the type II errors. The details about each function and the perturbations used are described in Sections 3.1–3.3. We report and discuss the results for all the case studies together after that.

3.1 Function as a sample from a GP

In the first simulation study, we sample the true function from a GP with zero mean and squared exponential covariance function. Since we are also using a squared exponential covariance for our method, this simulation study only focuses on the effectiveness of the proposed hypothesis testing when there is no model misspecification. We consider one dimensional input $x \in [0, 1]$. The model can be described as follows:

$$\begin{aligned} y &= f(x) + \epsilon, \\ f(x) &\sim \mathcal{GP}(0, k(x, x')), \\ \epsilon &\sim \mathcal{N}(0, \sigma_\epsilon^2). \end{aligned}$$

The squared exponential covariance function has the following form:

$$k(x, x') = \sigma_f^2 \exp\left(-\left[\frac{x - x'}{\theta}\right]^2\right).$$

The hyperparameters for the covariance function, $k(x, x')$, are set to $\sigma_f = 5$, and $\theta = 0.2$. The

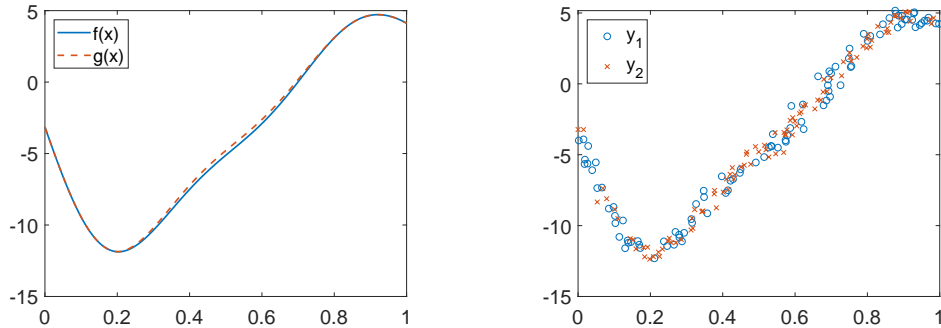


Figure 1: Plots for GP sample. Left panel: $f(x)$ and its perturbation, $g(x)$; Right panel: Noisy realizations from $f(x)$ and $g(x)$.

standard deviation of the noise, σ_ϵ , is set to 0.5. For each simulation run, a different sample is generated from the given GP model, and the estimated type I error is the percentage of runs for which the null hypothesis is rejected. For estimating the type II error, we create a perturbation $g(x)$ in the following way.

$$g(x) = \begin{cases} f(x) + \frac{1}{3} \sin\left(\pi\left(\frac{x-0.2}{0.8-0.2}\right)\right), & x \in [0.2, 0.8], \\ f(x), & \text{otherwise.} \end{cases}$$

The functions $f(x)$ and $g(x)$ sampled for one of the simulation runs (left panel), along with two noisy datasets generated from it (right panel) are shown in Figure 1.

3.2 Piston simulation function

The piston simulation function, as the name suggests, is used to simulate the motion of a piston inside an engine. This function was proposed by Kenett and Zacks (1998). This function was used by Ben-Ari and Steinberg (2007) to compare the performance of kriging with other methods in computer experiments. The response is the cycle time in seconds, i.e. the time required to complete

one cycle, and is given by:

$$f(x) = 2\pi \sqrt{\frac{M}{k + S^2 \frac{P_0 V_0 T_a}{T_0 V^2}}},$$

where

$$V = \frac{S}{2k} \left(\sqrt{A^2 + 4k \frac{P_0 V_0 T_a}{T_0}} - A \right),$$

$$A = P_0 S + 19.62M - \frac{kV_0}{S},$$

where M is the weight of the piston (kg), k is the coefficient of the spring, S is the piston surface area (m^2), P_0 is the atmospheric pressure (N/m^2), V_0 is the initial gas volume (m^3), T_0 is the filling gas temperature (K), and T_a is the ambient temperature (K). The number of input variables in this function are seven. We only choose two of them, V_0 and T_0 , as input variables. The other variables are fixed. A perturbation on the function, $g(x)$, is obtained by changing the value of one of the fixed variables, k , which is the spring coefficient. Figure 2 presents $f(x)$ and its perturbation, $g(x)$. It also shows the plots for the noisy datasets obtained from the original and perturbed functions. One can see that the differences between the functions are small and get masked visually in the noisy data.

3.3 Borehole function

The borehole function is used to model the flow of water through a borehole. This function has been widely used for computer experiments. See, for example, Harper and Gupta (1983), Morris et al. (1993), Zhou et al. (2011), Gramacy and Lian (2012), and Xiong et al. (2013). The response for this function is the water flow rate in the unit of $m^3/year$, given by:

$$f(x) = \frac{2\pi T_u (H_u - H_l)}{\ln(r/r_w) \left(1 + \frac{2LT_u}{\ln(r/r_w)r_w^2 K_w} + \frac{T_u}{T_l} \right)},$$

where r_w is the radius of the borehole (m), r is the radius of the influence (m), L is the length of the borehole (m), T_u is the transmissivity of the upper aquifer ($m^2/year$), T_l is the transmissivity of the lower aquifer ($m^2/year$), H_u is the potentiometric head of the upper aquifer (m), H_l is the

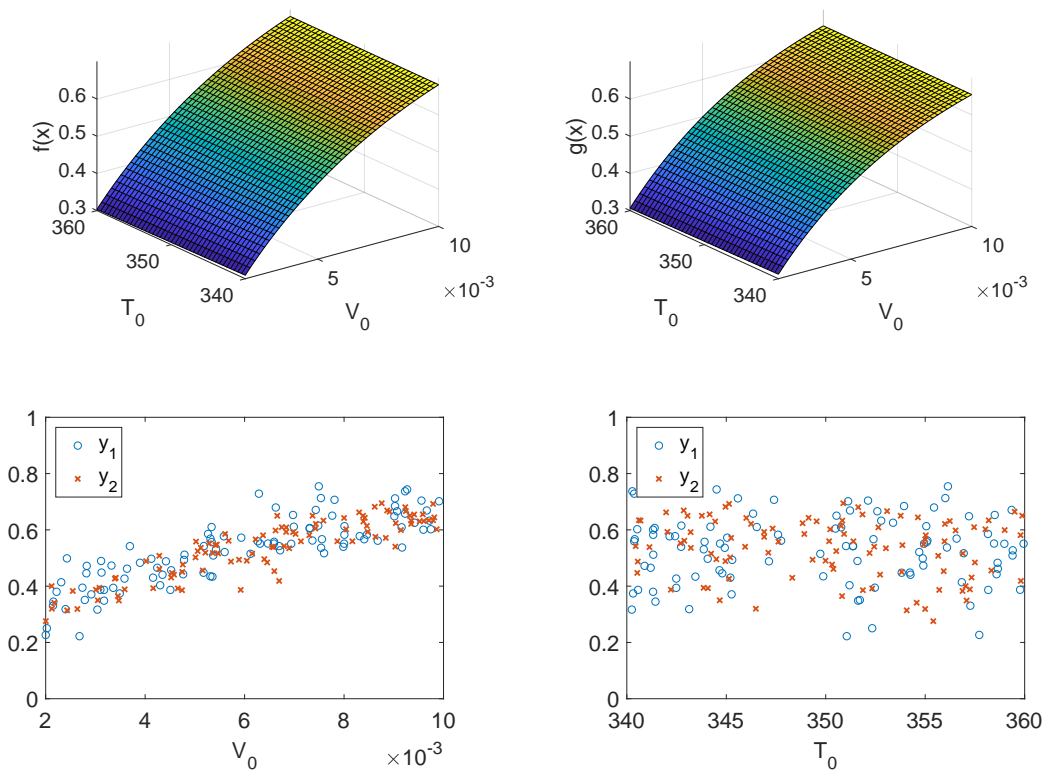


Figure 2: Plots for the piston function. Top left: $f(x)$; Top right: $g(x)$; Bottom left: noisy responses versus V_0 ; Bottom right: noisy responses versus T_0 .

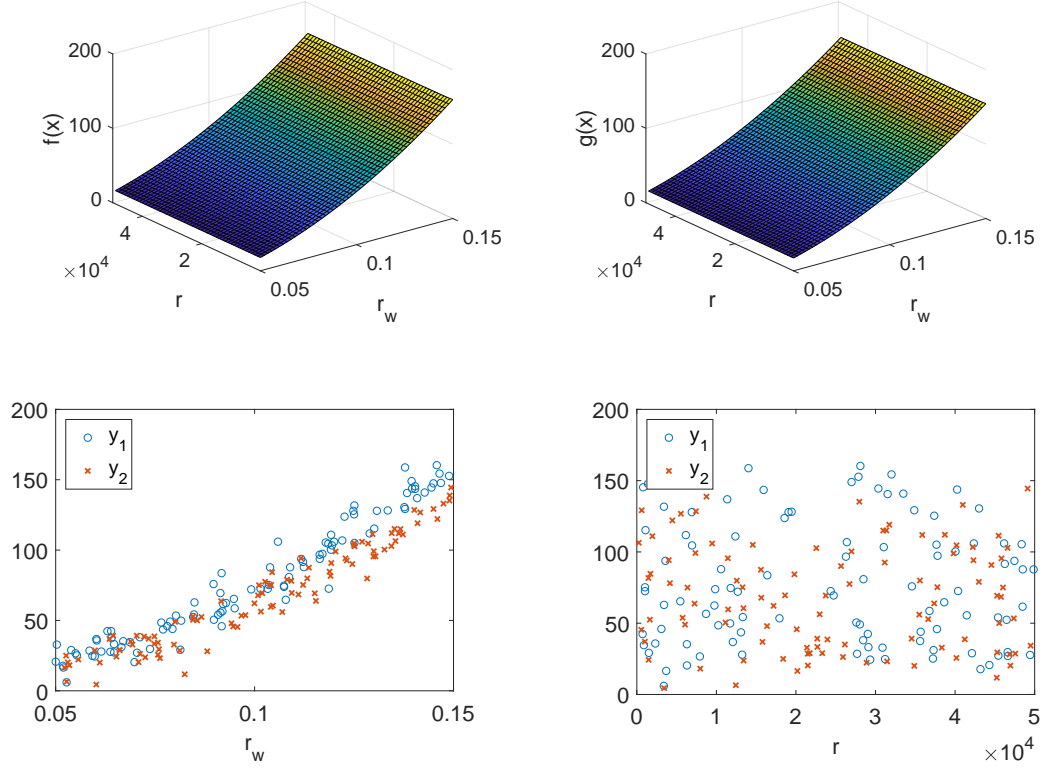


Figure 3: Plots for the borehole function. Top left: $f(x)$; Top right: $g(x)$; Bottom left: noisy responses versus r_w ; Bottom right: noisy responses versus r .

potentiometric head of the lower aquifer (m), and K_w is the hydraulic conductivity of the borehole ($m/year$). The number of input variables for the borehole function is eight. Again, we only consider two input variables (r and r_w) while fixing others. In this simulation study, a perturbation, $g(x)$, is obtained by changing the value of L , the length of the borehole. Figure 3 show the functions and the noisy data plots. Similar to the piston function study, this simulation study also sees a small difference between the function and its perturbation $g(x)$.

3.4 Results

Table 1 shows the estimated type I and type II errors for all the simulation studies, along with the L_2 distance of the perturbation $g(x)$ from $f(x)$. The L_2 distance varies between 4 to 7 %. For the first case study, when the true functions are GP samples, the estimated type I error is very close to the nominal level of 0.05 (5%). In the other two simulation studies, the estimated type I error is not as close to the nominal value as the first simulation study. This can be attributed to the fact that the form of the mean and covariance function required to sample these functions from a GP is not known and we use approximations in these studies. The agreement between the estimated type I error and the nominal value would depend on how well the GP approximates the function. If it is difficult to approximate a function using a known parametric covariance function, we can either come up with a more sophisticated mean and covariance function, or we can increase the confidence level of the test to a value greater than the desired level to account for model uncertainty.

By examining the type II error, we are satisfied that the method can identify the difference in the underlying functions even with small perturbations. Next, we apply our method to some real wind turbine datasets and compare the results with some of the existing works.

Table 1: Results for Type I and Type II error for simulated functions.

Function	Type I error	Type II error	L_2 dist %
GP sample	0.051	0.043	4.6
Piston	0.037	0.016	3.8
Borehole	0.077	0.006	6.6

4 Application

In this section, we demonstrate the application of the funGP method to a wind energy problem. Oftentimes, the wind farm owners and operators are interested in understanding the performance of a wind turbine. A common technique to characterize the performance of a wind turbine is through the use of its power curve (Ding, 2019, Chapters 5 and 6). A univariate power curve is the functional curve with wind speed as input and the generated wind power as output. But researchers realize that the wind power output is affected by other inputs more than just wind speed. Consequently,

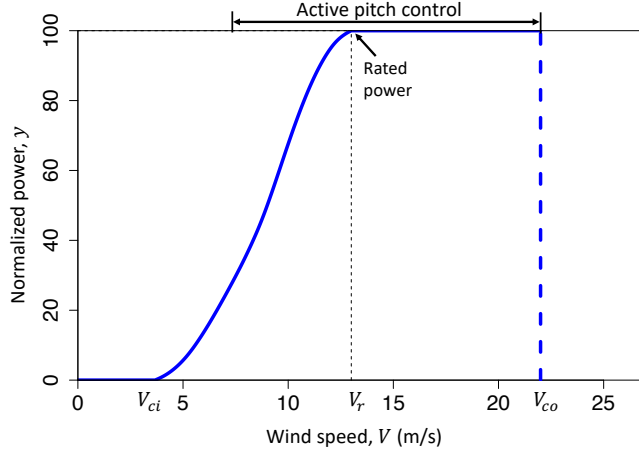


Figure 4: A nominal wind power curve. V_{ci} : the cut-in wind speed, V_r : the rated wind speed; V_{co} : the cut-out wind speed.

multivariate power curves have been developed; see, for instance, Chapter 5 of Ding (2019) or Lee et al. (2015).

A nominal wind power curve is shown in Figure 4. The turbine does not produce power below the cut-in wind speed V_{ci} . Above the cut-in speed, the power gradually rises till the rated power, and then its power output is capped at the rated power till the cut-out wind speed V_{co} , at which the turbine operation is stopped in order to protect components against damage. The pitch control is one of the main mechanisms to regulate a wind turbine’s power output (Senjyu et al., 2006); in Figure 4, we mark the wind speed region where the pitch control is active.

The power curve (univariate or multivariate) is generally learned through data; please see Chapter 5 of Ding (2019) for various methods. If one wants to compare the performance of two turbines or the same turbine over multiple time periods, they can do so by comparing the learned power curves. This raises a question that whether the difference in the learned curves is due to the randomness in the samples, and the noise, or the difference is genuine in turbine performance beyond random fluctuation. Our proposed method can hence be employed to answer this question. If the difference in the power curve is statistically insignificant at a given confidence level, then we can say that the power curves are statistically the same, and any difference observed in the learned curves is due to

the randomness in samples.

We apply our method to the four datasets as used by Hwangbo et al. (2017), which also constitutes a large portion of Chapter 6 of Ding (2019), and we download the four datasets from the book website of Ding (2019). Each dataset corresponds to a different turbine. The four turbines are labeled as WT1, WT2, WT3, and WT4. The datasets WT1 and WT2 are from onshore turbines and have the following five input variables: wind speed (V), wind direction (D), air density (ρ), turbulence intensity (I), and wind shear (S). The other two datasets (WT3 and WT4) correspond to offshore wind turbines with the input variable S replaced with humidity (H) and the rest of the variables same as that of the onshore turbines. Each of the four datasets comprises four years of data. We conduct a year to year comparison for each turbine, as done in Hwangbo et al. (2017). For this reason, each turbine’s dataset is divided into four annual datasets.

The marginal distributions of the covariates are different for each year, thus before computing their metric, Hwangbo et al. (2017) apply a method called covariate matching to the annual datasets. Covariate matching tries to match the marginal distributions of all the available environmental variables among the annual datasets by selecting the proper data subsets. Covariate matching is applied here in order to enable a fair comparison in turbine performance by ensuring that the distributions of the environmental variables are similar. We follow the same strategy with the same specifications as given in Hwangbo et al. (2017). After the covariate matching, Hwangbo et al. (2017) uses only the wind speed as the input variable to estimate the power curve. We also proceed in a similar way. In other words, we have wind speed as the input and wind power as the output. We input these datasets to our funGP algorithm and do a pairwise comparison between the annual datasets for each turbine using the following specification. We select a regular grid of 1,000 points from the range of the input variable (wind speed) and test the difference between underlying curves for any two annual datasets for a given turbine. A typical wind turbine operates at wind speeds between 5 m/s to 15 m/s for most of the time. Thus, we select this range to test the difference. Hwangbo et al. (2017) developed a 90 % confidence interval for their performance metric using bootstrap method. For comparison, we also build a 90 % confidence band on the difference of the power curves.

The outputs from our method is the pointwise difference in the power curves and the 90 % confidence band on the difference, for the power curves to be the same. In Table 2, we report the percentage of points, out of the 1,000 test points, for which the difference between two given yearly datasets is statistically significant. Whenever the percentage is greater than zero, we claim that the difference between corresponding two curves is statistically significant.

Speaking of the current industry practice for turbine performance comparison in the wind energy sector, the most popular method is to compare their peak power coefficient estimated from the data (IEC, 2005). The power coefficient, C_p , of a turbine is computed by using the following formula:

$$C_p = \frac{2y}{\rho AV^3},$$

where y is the wind power output and A is the sweeping area of the turbine blades. Here C_p is not a constant but rather a function of wind speed and a few other factors. The exact formula linking C_p to other physical variables does not exist. So it is empirically estimated. Using a functional C_p is not easy, and because of that, practitioners simply choose the peak value on the C_p -versus-wind-speed curve to represent the performance of a turbine. The power coefficient has a theoretical upper bound, known as the Betz limit, which is 0.593 (Ding, 2019) but the practical C_p is generally smaller than 0.5. It is obvious that this C_p metric is just a point metric of an otherwise functional difference.

Hwangbo et al. (2017) suggested another technique to compare the performance of wind turbines using the concepts of production economics. They devise a performance metric called productive efficiency which takes into account the overall power curve and not just the peak performance. But their final output is again a point metric of the functional differences, much like the power coefficient.

Table 2: Percentage of test points with statistically significant difference between annual datasets.

Turbine	Year 1 & 2	Year 1 & 3	Year 1 & 4	Year 2 & 3	Year 2 & 4	Year 3 & 4
WT1	54.8	57.7	54.5	9.8	0	0
WT2	42.4	41.7	42.6	0	0	1.9
WT3	86.6	81.6	75.4	56.2	76.9	40.5
WT4	78.6	62.6	66.3	37.8	56.9	0

Hwangbo et al. (2017)’s study find the productive efficiency metric has a good similarity with the power coefficient metric, although not exactly the same. Using the four datasets mentioned above, the performance quantifications using the two metrics registered a correlation of 0.75 (Hwangbo et al., 2017). Other than being a point metric, both the power coefficient and the productive efficiency methods do not quantify the estimation uncertainty on their own—one can go through an expensive bootstrap approach to get a confidence interval on the performance metrics. The funGP method, on the other hand, can lead to any level of confidence bands on the difference of the performance.

We compare our results with the metrics—the peak power coefficient and the productive efficiency—obtained by Hwangbo et al. (2017, Table II). We illustrate the comparison in a chart (see Figure 5) using vertical and horizontal lines with the following criteria:

- If the two metrics used by Hwangbo et al. (2017) agree with each other, and they also agree with our result (i.e., they both say the two annual periods are different or they both say the same), then we use vertical lines to demonstrate that.
- If the two metrics do not agree with each other, but one of them agree with our result, we still use vertical lines.
- However, if the two metrics agree with each other, but they do not agree with our method we use horizontal lines to show that.

In other words, the vertical lines imply an agreement between our method and at least one of the two metrics, where as the horizontal lines mean a disagreement between the two metrics and the funGP method. We observe that when the difference between two power curves is statistically significant, the confidence intervals of the peak power coefficient or the productive efficiency for the same two curves tend not to overlap, leading naturally to the overwhelming agreement pattern observed in Figure 5.

There are two comparison outcomes for which using funGP and either metric in Hwangbo et al. (2017) disagree: One is WT1 for Year 2 versus Year 3 and the other is WT2 for Year 3 versus Year 4. Taking a closer look reveals that the percentages of test points where the two curves are different, as reported in Table 2, are 9.8% and 1.9%, respectively, for these two cases. These two percentages are

Turbine	Year 1 & 2	Year 1 & 3	Year 1 & 4	Year 2 & 3	Year 2 & 4	Year 3 & 4
WT1	Vertical lines	Vertical lines	Vertical lines	Horizontal lines	Vertical lines	Vertical lines
WT2	Vertical lines	Vertical lines	Vertical lines	Vertical lines	Vertical lines	Horizontal lines
WT3	Vertical lines	Vertical lines	Vertical lines	Vertical lines	Vertical lines	Vertical lines
WT4	Vertical lines	Vertical lines	Vertical lines	Vertical lines	Vertical lines	Vertical lines

Figure 5: Comparison chart for the results obtained using funGP method to that of the peak power coefficient and the productive efficiency method. Vertical lines imply that the results agree. Horizontal lines imply that the results differ.

much smaller than the percentage values in other cases for which two curves are declared different. When we look at the power coefficient and productive efficiency values in Hwangbo et al. (2017, Table II), they are as such:

- WT 1’s power coefficient. Year 2: 0.388 with the 90% confidence intervals as [0.386, 0.392], and Year 3: 0.393 with the 90% confidence intervals as [0.390, 0.397].
- WT1’ productive efficiency. Year 2: 0.969 with the 90% confidence intervals as [0.966, 0.973], and Year 3: 0.972 with the 90% confidence intervals as [0.969, 0.975].
- WT2’s power coefficient. Year 3: 0.463 with the 90% confidence intervals as [0.460, 0.468], and Year 4: 0.462 with the 90% confidence intervals as [0.457, 0.467].
- WT2’s productive efficiency. Year 3: 0.970 with the 90% confidence intervals as [0.963, 0.973], and Year 4: 0.968 with the 90% confidence intervals as [0.962, 0.971].

Apparently, for the power coefficient and productive efficiency metrics, their 90% confidence intervals are only marginally overlapping, not really contradicting with the small regions of difference detected by using the funGP method. It is not unreasonable to consider that the funGP method is more sensitive to the difference between the two curves.

The funGP method provides a quantification of the regions of difference. Better yet, funGP can be used to compute the difference in the power curves at any point in the domain of the curve, and thus, gives a more detailed picture of the difference between any two curves, so that practitioners can see where the regions of difference are and thus make an informed decision regarding whether

the small difference regions matter or not. Figure 6 shows this difference vs wind speed plot for all the annual datasets for the first turbine (WT1).

Knowing the regions of difference has other benefits. It is helpful in deciding the maintenance plan for the turbine. For instance, if the difference occur in low power range, one may not necessarily need to go for expensive maintenance as doing so is unlikely to result in large change in the power output. Another important implication of knowing the difference regions is to decide the pitch control configuration of the turbine. As Creaby et al. (2009) explains, wind turbines aerodynamic characteristics change with time because of surface wear, dirt and other factors. Therefore, knowing the region of difference can help adjust the control laws to optimize the pitch control for different regions of operations, in order to maximize the power output. The funGP method is better suited in this application as a more powerful and informative testing and comparison method.

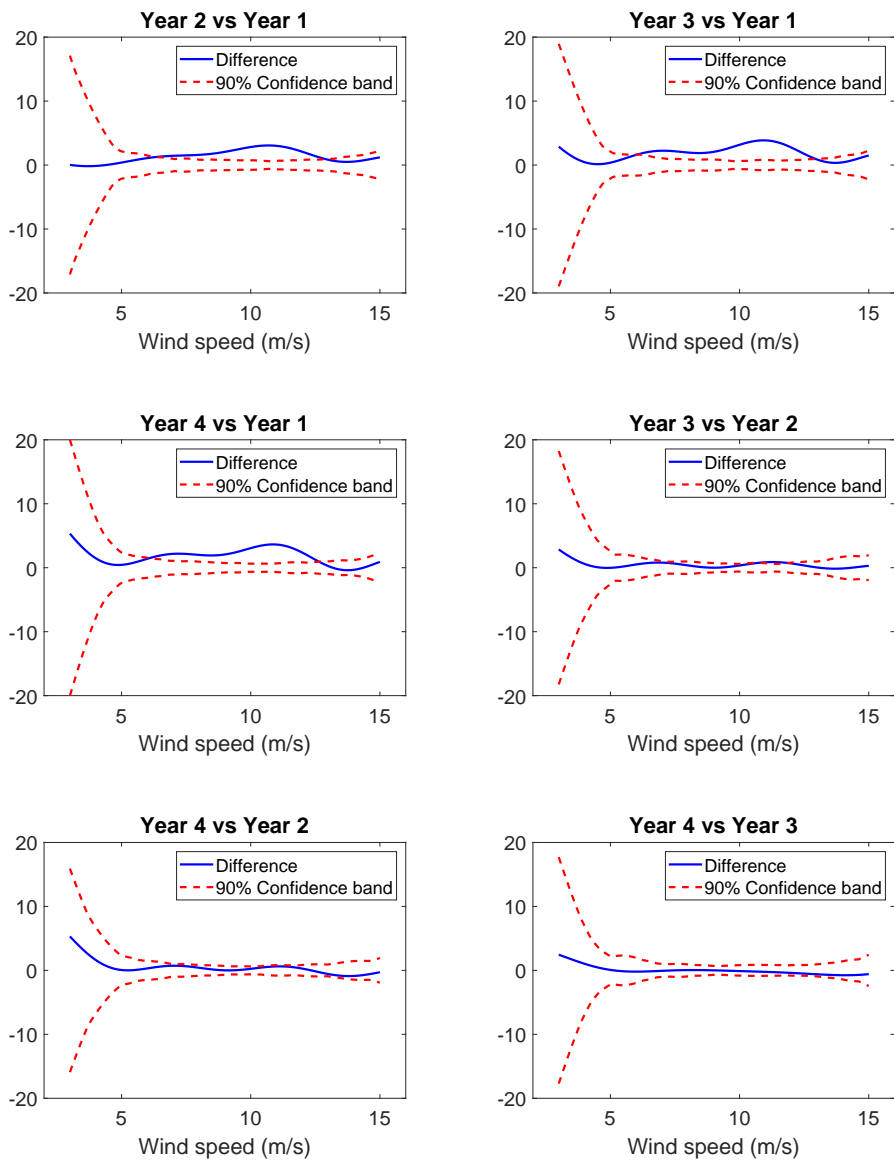


Figure 6: Difference in curves vs wind speed for WT1.

5 Discussions

In this work we propose a novel method to compare the underlying functions based on noisy datasets. The novelty of the method lies in its ability to produce a confidence band for the cases when the datasets do not have common input points and replicates. These datasets naturally occur in wind energy system where one cannot control the input points. Yet, one would like to do a comparison between the underlying functions generating these datasets. The funGP method comes very handy in these applications.

While the motivation for the method stemmed from wind power curve comparison, we believe that the method can be applied to many in other applications where the input points cannot be controlled. The method is particularly useful in lower dimension to visualize the difference between the function curves and understand how the functions differ in specific areas of input domain. This can be a useful tool as in the case of wind power curve where it can help devise control strategies for the turbine.

In the current framework, we use regularly spaced input points to do the comparison of the curves. In the higher dimensions, these numbers can grow quickly and may become computationally burdensome. Thus, one of the future directions of the work can be to use the minimum number of comparison points—based on the characteristics of the function under study—in order to reduce the computation time.

Acknowledgment

Ding’s research is partially supposed by NSF grants IIS-1741173 and CCF-1934904. Tuo’s research is supported by NSF DMS-1914636.

References

Ben-Ari, E. N. and Steinberg, D. M. (2007). Modeling data from computer experiments: An empirical comparison of kriging with MARS and projection pursuit regression. *Quality Engineering*, 19(4):327–338.

- Cox, D. and Lee, J. S. (2008). Pointwise testing with functional data using the Westfall–Young randomization method. *Biometrika*, 95(3):621–634.
- Creaby, J., Li, Y., and Seem, J. E. (2009). Maximizing wind turbine energy capture using multi-variable extremum seeking control. *Wind Engineering*, 33(4):361–387.
- Delgado, M. A. (1993). Testing the equality of nonparametric regression curves. *Statistics & Probability Letters*, 17(3):199–204.
- Ding, Y. (2019). *Data Science for Wind Energy*. Chapman & Hall/CRC Press, Boca Raton, FL.
- Fan, J. and Lin, S.-K. (1998). Test of significance when data are curves. *Journal of the American Statistical Association*, 93(443):1007–1021.
- Fisher, R. A. (1925). Application of “Student’s” distribution. *Metron*, 5:90–104.
- Gramacy, R. B. and Lian, H. (2012). Gaussian process single-index models as emulators for computer experiments. *Technometrics*, 54(1):30–41.
- Hall, P. and Hart, J. D. (1990). Bootstrap test for difference between means in nonparametric regression. *Journal of the American Statistical Association*, 85(412):1039–1049.
- Harper, W. and Gupta, S. (1983). Sensitivity/uncertainty analysis of a borehole scenario comparing Latin hypercube sampling and deterministic sensitivity approaches. Technical report, BMI/ONWI-516, Office of Nuclear Waste Isolation, Battelle Memorial Institute, Columbus, OH.
- Hotelling, H. (1931). The generalization of Student’s ratio. *The Annals of Mathematical Statistics*, 2(3):360–378.
- Hwangbo, H., Johnson, A., and Ding, Y. (2017). A production economics analysis for quantifying the efficiency of wind turbines. *Wind Energy*, 20(9):1501–1513.
- IEC (2005). *International Electrotechnical Commission 61400-12-1 Ed. 1, Wind Turbines-Part 12-1: Power Performance Measurements of Electricity Producing Wind Turbines*. Geneva, Switzerland.
- Kenett, R. S. and Zacks, S. (1998). *Modern Industrial Statistics: The Design and Control of Quality and Reliability*. Duxbury Press, Pacific Grove, CA.
- King, E., Hart, J. D., and Wehrly, T. E. (1991). Testing the equality of two regression curves using linear smoothers. *Statistics & Probability Letters*, 12(3):239–247.
- Kulasekera, K. B. (1995). Comparison of regression curves using quasi-residuals. *Journal of the American Statistical Association*, 90(431):1085–1093.

- Kulasekera, K. B. and Wang, J. (1997). Smoothing parameter selection for power optimality in testing of regression curves. *Journal of the American Statistical Association*, 92(438):500–511.
- Lee, G., Ding, Y., Genton, M. G., and Xie, L. (2015). Power curve estimation with multivariate environmental factors for inland and offshore wind farms. *Journal of the American Statistical Association*, 110(509):56–67.
- Morris, M. D., Mitchell, T. J., and Ylvisaker, D. (1993). Bayesian design and analysis of computer experiments: Use of derivatives in surface prediction. *Technometrics*, 35(3):243–255.
- Munk, A. and Dette, H. (1998). Nonparametric comparison of several regression functions: exact and asymptotic theory. *The Annals of Statistics*, 26(6):2339–2368.
- Neumeier, N. and Dette, H. (2003). Nonparametric comparison of regression curves: an empirical process approach. *The Annals of Statistics*, 31(3):880–920.
- Rasmussen, C. E. and Williams, C. K. I. (2006). *Gaussian Processes for Machine Learning*. The MIT Press.
- Senjyu, T., Sakamoto, R., Urasaki, N., Funabashi, T., Fujita, H., and Sekine, H. (2006). Output power leveling of wind turbine generator for all operating regions by pitch angle control. *IEEE Transactions on Energy conversion*, 21(2):467–475.
- Westfall, P. H. and Young, S. S. (1993). *Resampling-Based Multiple Testing: Examples and Methods for p-Value Adjustment*. John Wiley & Sons, New York, NY.
- Xiong, S., Qian, P. Z. G., and Wu, C. F. J. (2013). Sequential design and analysis of high-accuracy and low-accuracy computer codes. *Technometrics*, 55(1):37–46.
- Zhou, Q., Qian, P. Z. G., and Zhou, S. (2011). A simple approach to emulation for computer models with qualitative and quantitative factors. *Technometrics*, 53(3):266–273.

Appendix

A.1 Derivation for $\mathbf{C}(\mathbf{X}_{test}, \mathbf{X}_{test})$

The predictive mean vector for $f_1(\cdot)$ given \mathcal{D}_1 for all the points \mathcal{T} is as follows:

$$\hat{\mathbf{f}}_1 = \mathbf{K}(\mathbf{X}_{test}, \mathbf{X}^{(1)})[\mathbf{K}(\mathbf{X}^{(1)}, \mathbf{X}^{(1)}) + \sigma_\epsilon^2 \mathbf{I}_{n_1}]^{-1} \mathbf{y}^{(1)}.$$

Similarly, the predictive mean vector for $f_2(\cdot)$ conditioned on \mathcal{D}_2 for all the points \mathcal{T} is given by:

$$\hat{\mathbf{f}}_2 = \mathbf{K}(\mathbf{X}_{test}, \mathbf{X}^{(2)})[\mathbf{K}(\mathbf{X}^{(2)}, \mathbf{X}^{(2)}) + \sigma_\epsilon^2 \mathbf{I}_{n_2}]^{-1} \mathbf{y}^{(2)}.$$

Thus $\mathbf{C}(\mathbf{X}_{test}, \mathbf{X}_{test}) = Cov(\hat{\mathbf{f}}_2 - \hat{\mathbf{f}}_1)$ is expressed as follows:

$$\begin{aligned} & Cov(\hat{\mathbf{f}}_2 - \hat{\mathbf{f}}_1) \\ &= Cov(\mathbf{K}(\mathbf{X}_{test}, \mathbf{X}^{(2)})[\mathbf{K}(\mathbf{X}^{(2)}, \mathbf{X}^{(2)}) + \sigma_\epsilon^2 \mathbf{I}_{n_2}]^{-1} \mathbf{y}^{(2)} - \mathbf{K}(\mathbf{X}_{test}, \mathbf{X}^{(1)})[\mathbf{K}(\mathbf{X}^{(1)}, \mathbf{X}^{(1)}) + \sigma_\epsilon^2 \mathbf{I}_{n_1}]^{-1} \mathbf{y}^{(1)}) \\ &= Var(\mathbf{K}(\mathbf{X}_{test}, \mathbf{X}^{(2)})[\mathbf{K}(\mathbf{X}^{(2)}, \mathbf{X}^{(2)}) + \sigma_\epsilon^2 \mathbf{I}_{n_2}]^{-1} \mathbf{y}^{(2)}) \\ &+ Var(\mathbf{K}(\mathbf{X}_{test}, \mathbf{X}^{(1)})[\mathbf{K}(\mathbf{X}^{(1)}, \mathbf{X}^{(1)}) + \sigma_\epsilon^2 \mathbf{I}_{n_1}]^{-1} \mathbf{y}^{(1)}) \\ &- 2 Cov(\mathbf{K}(\mathbf{X}_{test}, \mathbf{X}^{(2)})[\mathbf{K}(\mathbf{X}^{(2)}, \mathbf{X}^{(2)}) + \sigma_\epsilon^2 \mathbf{I}_{n_2}]^{-1} \mathbf{y}^{(2)}, \mathbf{K}(\mathbf{X}_{test}, \mathbf{X}^{(1)})[\mathbf{K}(\mathbf{X}^{(1)}, \mathbf{X}^{(1)}) + \sigma_\epsilon^2 \mathbf{I}_{n_1}]^{-1} \mathbf{y}^{(1)}) \\ &= \mathbf{K}(\mathbf{X}_{test}, \mathbf{X}^{(2)})[\mathbf{K}(\mathbf{X}^{(2)}, \mathbf{X}^{(2)}) + \sigma_\epsilon^2 \mathbf{I}_{n_2}]^{-1} Var(\mathbf{y}^{(2)}) [\mathbf{K}(\mathbf{X}^{(2)}, \mathbf{X}^{(2)}) + \sigma_\epsilon^2 \mathbf{I}_{n_2}]^{-1} \mathbf{K}(\mathbf{X}_{test}, \mathbf{X}^{(2)})^\top \\ &+ \mathbf{K}(\mathbf{X}_{test}, \mathbf{X}^{(1)})[\mathbf{K}(\mathbf{X}^{(1)}, \mathbf{X}^{(1)}) + \sigma_\epsilon^2 \mathbf{I}_{n_1}]^{-1} Var(\mathbf{y}^{(1)}) [\mathbf{K}(\mathbf{X}^{(1)}, \mathbf{X}^{(1)}) + \sigma_\epsilon^2 \mathbf{I}_{n_1}]^{-1} \mathbf{K}(\mathbf{X}_{test}, \mathbf{X}^{(1)})^\top \\ &- 2 \mathbf{K}(\mathbf{X}_{test}, \mathbf{X}^{(2)})[\mathbf{K}(\mathbf{X}^{(2)}, \mathbf{X}^{(2)}) + \sigma_\epsilon^2 \mathbf{I}_{n_2}]^{-1} Cov(\mathbf{y}^{(2)}, \mathbf{y}^{(1)}) [\mathbf{K}(\mathbf{X}^{(1)}, \mathbf{X}^{(1)}) + \sigma_\epsilon^2 \mathbf{I}_{n_1}]^{-1} \mathbf{K}(\mathbf{X}_{test}, \mathbf{X}^{(1)})^\top \\ &= \mathbf{K}(\mathbf{X}_{test}, \mathbf{X}^{(2)})[\mathbf{K}(\mathbf{X}^{(2)}, \mathbf{X}^{(2)}) + \sigma_\epsilon^2 \mathbf{I}_{n_2}]^{-1} \mathbf{K}(\mathbf{X}_{test}, \mathbf{X}^{(2)})^\top \\ &+ \mathbf{K}(\mathbf{X}_{test}, \mathbf{X}^{(1)})[\mathbf{K}(\mathbf{X}^{(1)}, \mathbf{X}^{(1)}) + \sigma_\epsilon^2 \mathbf{I}_{n_1}]^{-1} \mathbf{K}(\mathbf{X}_{test}, \mathbf{X}^{(1)})^\top \\ &- 2 \mathbf{K}(\mathbf{X}_{test}, \mathbf{X}^{(2)})[\mathbf{K}(\mathbf{X}^{(2)}, \mathbf{X}^{(2)}) + \sigma_\epsilon^2 \mathbf{I}_{n_2}]^{-1} \mathbf{K}(\mathbf{X}^{(2)}, \mathbf{X}^{(1)}) [\mathbf{K}(\mathbf{X}^{(1)}, \mathbf{X}^{(1)}) + \sigma_\epsilon^2 \mathbf{I}_{n_1}]^{-1} \mathbf{K}(\mathbf{X}_{test}, \mathbf{X}^{(1)})^\top. \end{aligned}$$

A.2 Karhunen-Loève expansion of a Gaussian process

Karhunen-Loève expansion provides a framework to decompose any stochastic process as an infinite sum of basis functions. Since, we are interested in Gaussian processes, we will discuss the KL expansion only for GPs. Let us now consider that $f(\mathbf{x})$ is a zero mean Gaussian process with

$k(\mathbf{x}, \mathbf{x}')$ as the covariance function. This process can be decomposed as follows:

$$f(\mathbf{x}) = \sum_{k=1}^{\infty} \sqrt{\lambda_k} \phi_k(\mathbf{x}) z_k, \quad (10)$$

where $z_k \mid k = 1 \dots \infty$ are the uncorrelated standard normal random variables; and $\phi_k(\cdot) \mid k = 1 \dots \infty$ are the basis functions. The value of λ_k and $\phi_k(\cdot)$ can be obtained by solving the following integral eigenproblem

$$\int k(\mathbf{x}, \mathbf{x}') \phi(\mathbf{x}') d\mathbf{x}' = \lambda \phi(\mathbf{x}). \quad (11)$$

In practice, Equation (11) can be solved by discretizing the integral. Let us again assume that we have n data points from the process $f(x)$. Then, we consider the following matrix eigenproblem

$$\mathbf{K} \mathbf{u}_k = \lambda_k^{mat} \mathbf{u}_k, \quad (12)$$

where \mathbf{K} is again the covariance matrix with entries $\mathbf{K}_{ij} = k(\mathbf{x}_i, \mathbf{x}_j) \mid i, j = 1 \dots n$;

λ_k^{mat} are the eigenvalues of the covariance matrix \mathbf{K} ;

\mathbf{u}_k are the normalized unit eigenvectors of the covariance matrix \mathbf{K} .

The eigenvalues and eigenfunctions of the integral problem are related to the eigenvalues and eigenvectors of the matrix problem in the following way:

$$\lambda_k = \frac{\lambda_k^{mat}}{n}, \quad (13)$$

$$\phi_k(\mathbf{x}_j) = \sqrt{n} (\mathbf{u}_k)_j, \quad (14)$$

where $(\mathbf{u}_k)_j$ is the j^{th} component of the eigenvector \mathbf{u}_k . The above approximation reduces the infinite sum in the KL expansion to a finite sum (truncated KL expansion) as follows:

$$\begin{aligned} f(x_j) &\approx \sum_{k=1}^n \sqrt{\frac{\lambda_k^{mat}}{n}} \sqrt{n} (\mathbf{u}_k)_j z_k, \\ &= \sum_{k=1}^n \sqrt{\lambda_k^{mat}} (\mathbf{u}_k)_j z_k. \end{aligned} \quad (15)$$

This decomposition can be written compactly in the matrix form. If we consider a vector, $\mathbf{f} = (f(\mathbf{x}_1), f(\mathbf{x}_2), \dots, f(\mathbf{x}_n))^T$, then it can be decomposed as follows:

$$\mathbf{f} = \mathbf{U} \mathbf{\Lambda}^{\frac{1}{2}} \mathbf{z}, \quad (16)$$

where \mathbf{U} is the matrix with columns as eigenvectors of covariance matrix \mathbf{K} ; $\mathbf{\Lambda}$ is a diagonal matrix with eigenvalues of \mathbf{K} and \mathbf{z} is a vector of length n with uncorrelated standard normal random variables as its components.